Hindawi
International Journal of Aerospace Engineering
Volume 2022, Article ID 5419377, 15 pages
https://doi.org/10.1155/2022/5419377

Research Article

Finite-Time Attitude Tracking Control for Hypersonic Flight Vehicles with Actuator Saturation

Teng Cao, Huajun Gong, Huiyunuo Xiao, and Yixuan Xue

College of Automation Engineering, Nanjing University of Aeronautics and Astronautics, Nanjing 211106, China

Correspondence should be addressed to Huajun Gong; ghj301@nuaa.edu.cn

Received 8 April 2022; Revised 19 October 2022; Accepted 2 November 2022; Published 23 November 2022

Academic Editor: Guillermo Valencia-Palomo

This paper investigates finite-time attitude tracking control strategies for hypersonic flight vehicles (HFVs) with parameter uncertainties, external disturbances, and actuator saturations by applying sliding model control, adaptive mechanism, and nonlinear disturbance observer techniques. A nonlinear dynamic model of HFV attitude system in reentry flight phase is established. Then, a basic attitude control method of the HFV system is designed based on a terminal sliding mode control (TSMC) scheme to accommodate the system-lumped disturbance torques and guarantee the finite-time stability. To relax the prior knowledge of bounded lumped disturbance of the TSMC-based HFV attitude system, an adaptive TSMC (ATSMC) scheme is proposed. In order to relax the limit of compound uncertainties and attenuate chattering phenomenon of the TSMC-based HFV attitude system, a nonlinear disturbance observer-based TSMC (DO-TSMC) scheme is presented, which enhances the disturbance attenuation and robust tracking performance. Finally, simulation results of a generic X-33 nonlinear model exhibit the effectiveness of the proposed TSMC, ATSMC, and DO-TSMC schemes.

1. Introduction

Research on hypersonic flight vehicles (HFVs) is widely concerned in recent years due to its high-speed transportation, ability to accomplish modern space missions, and broad application in military and civil fields [1–4]. However, there exists many challenges to design control law for the HFV attitude system containing complex coupling terms, unknown disturbances, and uncertainty of external environment [5, 6]. Under the influence of inaccurate modeling and external disturbances, the control system may not be able to complete the scheduled task, or even out of control. Therefore, it is essential for us to propose efficient approaches to design the attitude system.

In recent years, there have been a lot of research results on hypersonic vehicle controller design with external disturbances and uncertainties. Sliding mode control (SMC) [7, 8], backstepping control [9], twisting control [10], adaptive control [11], coupling effect-triggered control (CETC) [12], and compound control methods of the ways mentioned above have been largely used to enhance the attitude control performance. In [13], a tracking control scheme with quantization mechanism, which uses an interval type-2 fuzzy neural network (IT2FNN) is proposed for HFVs. A coordinate-free, finite-time, attitude control is employed for thrust-vectoring spacecraft to guarantee the required thrust vector exactly at the predefined time [14]. In [15], under the condition of the inaccuracy of measured flight path angle, external disturbances, and actuator saturation, a backstepping-based control is developed for the tracking control of HFVs. In [16], the predefined-time adaptive fuzzy tracking control problem of HFVs is solved by a novel fuzzy adaptive control strategy based on fuzzy approximation and backstepping control techniques. To cope with tracking performance with uncertainties of HFVs, the article [17] explores a new adaptive fuzzy nonsmooth backstepping output-feedback control scheme.

On account of its fast global convergence, simple algorithm, high robustness against external perturbation, and system uncertainties, SMC has been extensively applied to compensate for the lumped disturbances. In order to improve the robust performance and obtain finite-time convergence, the terminal sliding mode (TSM) controller based on the backstepping frame is designed [18]. However, by reason of the difficulty to obtain the upper bound of uncertainty or disturbance in practice, compound control methods may lead to large

chattering phenomenon and energy loss. In [19], a method combined with TSMC and adaptive techniques is raised to overcome actuator faults, which ensures the system stable in the fixed time even under the condition of actuator faults and model uncertainties. An adaptation strategy is employed to estimate unknown information. In [20], the synthetic neural learning combined with the nonsingular second-order terminal sliding mode is raised to deal with model uncertainties for hypersonic reentry vehicle (HRV). In this paper, the influence value of system fault is obtained by RBF neural network mechanism. However, the disturbance in the system is not estimated. The disadvantage of this controller design method is that it needs to select a larger gain to ensure the disturbance and fault estimation error in the system, which will cause energy waste. In [21], a singular free fast terminal sliding mode controller is proposed for velocity subsystem of HFVs with multisource uncertainty and actuator fault. In order to attenuate chattering and compensate for the disturbances, the article [22] presents a novel fixed-time sliding mode disturbance observer (SMDO). In [23], a novel fixed-time convergent nonsmooth backstepping control scheme for air-breathing hypersonic vehicles through augmented sliding mode observers (ASMOs) is raised to solve uncertainty and measurement noise. It is worth noting that although references [21–23] use the scheme of disturbance observer to compensate the lumped disturbance value, the design of disturbance observer has certain limitations. For example, the disturbance should be differentiable and some observers require the disturbance to be constant or slowly varying. In reality, the disturbance or fault may not satisfy these assumptions. In [24], a novel learning observer-based control strategy is proposed for a faulty rigid spacecraft attitude system. The observer can estimate actuator fault that are constant, periodic, or aperiodically time-varying. In addition, because the actuator is constrained by its own physical conditions, we need to consider the case of actuator input saturation in the controller design process. Input saturation will seriously affect the performance of the control system, leading to system instability [25, 26]. In [27], the difference between the required control input and the actual control input is expressed as a known continuous function multiplied by an unknown constant vector. The adaptive technique is used to estimate the unknown vector, and then, a backstepping controller is designed to compensate the error value of control saturation. In order to further solve the problem of input saturation, reference [28] proposed a fast adaptive terminal sliding mode controller with antisaturation by introducing hyperbolic tangent function and auxiliary system, which can not only meet the physical constraints of the actuator but also ensure that the sliding mode manifold is finite-time stable. In [29], an adaptive fixed-time antisaturation control (AFAC) algorithm is proposed for FHV with actuator constraints. The adaptive law in controller is updated according to the deviation value of the control signal to improve the ability of the controller to suppress actuator saturation. However, the introduction of adaptive update increases the complexity of the controller. To the best of our knowledge, the results about the integrated attitude tracking control design for HFV system with time-varying disturbance and actuator saturation are limited, which remain challenging and motivate us to do this study.

In this paper, we focus on the attitude control problem of HFVs in reentry phase, where the model uncertainty, external disturbance, and actuator saturation are taken into account. In order to achieve the finite-time stability, the terminal sliding mode manifold is introduced. Assuming that there exists a prior knowledge of the bounded external disturbances and inertia uncertainties, a basic TSMC-based attitude control scheme is proposed. Further, an adaptive mechanism and a nonlinear disturbance observer are, respectively, designed for the TSMC-based attitude control system, which ensure the finite-time convergence in both reaching phase and sliding phase. Comparing with the results in the literature, the main contributions of this paper are as follows:

(1) A basic TSMC scheme is proposed for the HFV attitude system in the presence of model uncertainties, external disturbance, and actuator saturation. Compared with the conventional control methods, such as backstepping control [30] and integrated SMC [31, 32], the basic TSMC method can ensure the closed-loop attitude system to be asymptotically stable and track the reference signals in a finite time. Inspired by reference [32, 33], the TSMC control strategies with the low-pass filter are proposed to attenuate the chattering phenomenon caused by switching function. The discontinuous signal can be smoothed by the low-pass filter so the system can be stable with no chattering in the finite time. The stability of closed-loop attitude control system is analyzed using the Lyapunov method, and moreover, the system can be guaranteed to be finite-time stable

(2) To overcome the requirement of a prior knowledge of bounded lumped disturbance of the basic TSMC-based HFV attitude system, an adaptive law is introduced to adapt the switching gains, yielding an adaptive TSMC (ATSMC) scheme which is proposed. Compared with the conventional methods [32, 33], a suitable switching gain is selected according to the adaptive mechanism, which can reduce the large chattering phenomenon caused by the large gain

(3) To solve the limits of lumped disturbance and attenuate chattering phenomenon of the basic TSMC-based HFV attitude system, a nonlinear disturbance observer-based TSMC (DO-TSMC) is presented, which enhances the disturbance attenuation and robust performance. Compared with the existing adaptive SMC [31] and observer-based methods [34], the proposed DO-TSMC scheme relaxes the limits of uncertainties and disturbance and achieves higher precision, less chattering, faster finite-time convergence, and no need for prior knowledge of uncertainties. The class of disturbance considered in this paper can be much larger than the existing disturbance observer method [34]

This paper is organized as follows. In Section 2, the attitude control problem of the HFVs is formulated. In Section 3, the TSMC, ATSMC, and DO-TSMC-based attitude control

systems are designed, respectively. Simulation studies are given in Section 4 to demonstrate the effectiveness of the proposed schemes, followed by the conclusion of this study in Section 5.

2. Attitude Model and Control System Framework of HFVs

In this section, a dynamic model of HFVs with parameter uncertainty, external disturbance, and actuator saturation is given, and the attitude control system framework is designed.

2.1. HFV Attitude Dynamic Model

2.1.1. Generic Attitude Dynamic Model. The attitude dynamic equations of HFVs are given by

$$\begin{aligned} p &= \frac{I_{zz}M_x}{I_{xx}I_{zz}-I_{xz}^2} + \frac{I_{xz}M_z}{I_{xx}I_{zz}-I_{xz}^2} + \frac{(I_{xx}-\dot{I}_{yy}+I_{zz})I_{xz}}{I_{xx}I_{zz}-I_{xz}^2}pq + \frac{(I_{yy}-I_{zz})I_{zz}-I_{xz}^2}{I_{xx}I_{zz}-I_{xz}^2}qr, \\ q &= \frac{M_y}{I_{yy}} + \frac{I_{xz}}{I_{yy}}(r^2-p^2) + \frac{I_{zz}-I_{xx}}{I_{yy}}pr, \\ \dot{r} &= \frac{I_{xz}M_x}{I_{xx}I_{zz}-I_{xz}^2} + \frac{I_{xx}M_z}{I_{xx}I_{zz}-I_{xz}^2} + \frac{(I_{xx}-I_{yy})I_{xx}+I_{xz}^2}{I_{xx}I_{zz}-I_{xz}^2}pq + \frac{(I_{yy}-I_{xx}-I_{zz})I_xz}{I_{xx}I_{zz}-I_{xz}^2}qr, \end{aligned} \tag{1}$$

and the kinematic equations of HFVs are given by

$$\begin{aligned} \dot{\alpha} &= -p\cos\alpha\tan\beta + q - r\sin\alpha\tan\beta - \frac{\cos\phi}{\cos\beta}\left[\dot{\gamma} - \dot{\xi}\cos\chi - (\dot{\tau}+\Omega_E)\cos\xi\cos\chi\right] + \frac{\sin\phi}{\cos\beta}\left\{\dot{\chi}\cos\gamma - \dot{\xi}\sin\chi\sin\gamma + (\dot{\tau}+\Omega_E)(\cos\xi\cos\chi\sin\gamma - \sin\xi\cos\gamma)\right\}, \\ \dot{\beta} &= p\sin\alpha - r\cos\alpha + \sin\phi\left[\dot{\gamma} - \dot{\xi}\cos\chi + (\dot{\tau}+\Omega_E)\cos\xi\sin\chi\right] + \cos\phi\left[\dot{\chi}\cos\gamma - \dot{\xi}\sin\chi\sin\gamma - (\dot{\tau}+\Omega_E)\cos\xi\cos\chi\sin\gamma - \sin\xi\cos\gamma\right], \\ \dot{\phi} &= -p\cos\alpha\cos\beta - q\sin\beta - r\sin\alpha\cos\beta + \dot{\alpha}\sin\beta - \dot{\chi}\sin\gamma - \dot{\xi}\sin\chi\cos\gamma + (\dot{\tau}+\Omega_E)(\cos\xi\cos\chi\cos\gamma + \sin\xi\sin\gamma), \end{aligned} \tag{2}$$

where ϕ, α, and β are bank, attack, and sideslip angles; p, q, and r are roll, pitch, and yaw angular rates; χ, ξ, and τ are heading, latitude, and longitude angles; Ω_E is the Earth's angular rate; and the definitions of other variables are given in [31].

2.1.2. Attitude Dynamic Model in Reentry Phase. In the reentry flight phase, because the rotational motion of the HFVs in reentry phase is much faster than the rotational motion of the Earth, the angular velocity of the Earth Ω_E can be neglected, and the translational motion can hardly affect the rotational motion. The derivatives of both position and direction of velocity and the Earth's angular velocity are negligible with respect to the rotational motion. Therefore, Equation (2) can be simplified as

$$\begin{aligned} \alpha &= -p\cos\alpha\tan\beta + q - r\sin\alpha\tan\beta, \\ \beta &= p\sin\dot{\alpha} - r\cos\alpha, \\ \dot{\phi} &= -p\cos\alpha\cos\beta - q\sin\beta - r\sin\alpha\cos\beta. \end{aligned} \tag{3}$$

2.1.3. Uncertain Model with Disturbance. The reentry attitude dynamics of HFVs with parameter uncertainty and external disturbance can be described as

$$(I+\Delta I)\dot{\omega} = -\omega^{\times}(I+\Delta I)\omega + M + d, \tag{4}$$

where $\omega = [p, q, r]^T$ is the angular rate vector, $I \in R^{3\times3}$ is the inertia matrix, and $\Delta I \in R^{3\times3}$ is an uncertain part of the inertia matrix, which is caused by the fuel consumption and variations of particular payloads. $d = [d_1, d_2, d_3]^T$ is the external disturbance vector. $M = [M_x, M_y, M_z]^T$ is the control torque vector, which is calculated by

$$M = D(t)u, \tag{5}$$

where $D(t) \in R^{3\times m}$, m is the number of the control surfaces, and $u = [u_1, u_2, \cdots, u_m]^T$ is the vector of aerodynamic surface deflections. Then, the attitude dynamic model can be rewritten as

$$\begin{aligned} \dot{\Omega} &= R\omega, \\ \dot{\omega} &= -I^{-1}\omega^{\times}I\omega + I^{-1}Du + f_1, \end{aligned} \tag{6}$$

where $\Omega = [\phi, \alpha, \beta]^T$ is attitude angle vector, $f_1 = I^{-1}(d - \Delta I\dot{\omega} - \omega^{\times}\Delta I\omega)$, and the matrices R, I, and $\omega^{\times}$ are as

$$\begin{aligned} R &= \begin{bmatrix} -\cos\alpha\cos\beta & -\sin\beta & -\sin\alpha\cos\beta \\ -\cos\alpha\tan\beta & 1 & -\sin\alpha\tan\beta \\ \sin\alpha & 0 & -\cos\alpha \end{bmatrix}, \\ I &= \begin{bmatrix} I_{xx} & -I_{xy} & -I_{xz} \\ -I_{xy} & I_{yy} & -I_{yz} \\ -I_{xz} & -I_{yz} & I_{zz} \end{bmatrix}, \\ \omega^{\times} &= \begin{bmatrix} 0 & -r & q \\ r & 0 & -p \\ -q & p & 0 \end{bmatrix}. \end{aligned} \tag{7}$$

2.1.4. Uncertain Model with Disturbance and Actuator Saturation. Since there are input constraints on the control surfaces of HFVs, thus the attitude dynamic model (6) is

rewritten as

$$\begin{aligned}\dot{\Omega} &= R\omega,\\ \dot{\omega} &= -I^{-1}\omega^{\times}I\omega + I^{-1}D\mathrm{sat}(u) + f_1,\end{aligned} \tag{8}$$

where $\mathrm{sat}(u_i)$, $i = 1, 2, \cdots, m$ is defined as

$$\mathrm{sat}(u_i) = \begin{cases} \bar{u}_i, & u_i > \bar{u}_i,\\ u_i, & \underline{u}_i \le u_i \le \bar{u}_i,\\ \underline{u}_i, & u_i < \underline{u}_i. \end{cases} \tag{9}$$

Further, define an auxiliary variable $\delta = [\delta_1, \delta_2, \cdots, \delta_m]^T$ as

$$\delta_i = \begin{cases} \bar{u}_i - u_i, & u_i > \bar{u}_i,\\ 0, & \underline{u}_i \le u_i \le \bar{u}_i,\\ \underline{u}_i - u_i, & u_i < \underline{u}_i, \end{cases} \tag{10}$$

then (9) and (10) yield to

$$\mathrm{sat}(u) = \delta + u. \tag{11}$$

Substituting (11) into (8), the HFV attitude dynamic model with uncertainties, disturbances, and actuator input saturations can be expressed by

$$\begin{aligned}\dot{\Omega} &= R\omega,\\ \dot{\omega} &= -I^{-1}\omega^{\times}I\omega + I^{-1}Du + f,\end{aligned} \tag{12}$$

where $f = I^{-1}(d - \Delta I\dot{\omega} - \omega^{\times}\Delta I\omega) + I^{-1}(D\delta)$ and it can be considered as a lumped disturbance for HFV attitude dynamics.

2.2. Attitude Control Problem and Control System Framework

2.2.1. Control Objective. The control objective is to solve the attitude control problem of HFV system (12) with the parameter uncertainties, external disturbances, and control input constraints. An advanced control method is necessary to make the attitude system output Ω track a reference input Ω_r in the finite time.

2.2.2. Control Method Motivation. As a robust nonlinear control method, the SMC theory is applied in this control problem. Therefore, a basic TSMC scheme is designed, an ATSMC scheme is designed in which an adaptive law is used to estimate the upper bounds of the lumped disturbance, and finally, a DO-TSMC is designed in which a nonlinear disturbance observer is used to online estimate the value of lumped disturbances.

2.2.3. Control System Framework. A block diagram of the HFV attitude control system is designed as shown in Figure 1. It consists of two parts; the inner loop is the adaptive mechanism and disturbance estimation observer, while the outer loop is the basic TSMC-based attitude controller.

3. Finite-Time Attitude Controller Design

In this section, three finite-time attitude controllers based on the TSMC, ATSMC, and DO-TSMC schemes are designed for the HFV attitude system in the presence of model uncertainties, external disturbances, and actuator saturations.

3.1. Preliminaries

Assumption 1. The reference signal $\Omega_r = [\phi_r, \alpha_r, \beta_r]^T$ is bounded and continuously differentiable, and its derivative $\dot{\Omega}_r$ is bounded.

Assumption 2. The system-lumped disturbance torque f is bounded, and it satisfies $\|f\| \le l_d$, where $l_d > 0$ is a constant.

Assumption 3. The derivative of the system-lumped disturbance torque is bounded, and it satisfies $\|\dot{f}\| \le k_d$, where $k_d > 0$ is a constant.

Lemma 4 [35]. *Consider the nonlinear system described as $\dot{x} = f(x, u), f(0) = 0, x \in R^n$. Suppose $V(x)$ is a continuous positive definite function (defined on $D \in \mathfrak{R}$) and $\dot{V}(x) + \lambda V^{\rho}(x)$ is negative semidefinite on D for $0 < \rho < 1$ and $\lambda > 0$, then there exists an area $D_0 \in \mathfrak{R}$ such that any $V(x)$ which starts from $D_0 \in \mathfrak{R}$ can reach $V(x) \equiv 0$ in the finite time. Moreover, if T_{reach} is the time to reach $V(x) \equiv 0$, then*

$$T_{reach} \le \frac{V^{1-\rho}(x_o)}{\lambda(1-\rho)}, \tag{13}$$

where $V(x_0)$ is the initial value of $V(x)$.

Lemma 5 [36]. *Consider the nonlinear system described as $\dot{x} = f(x, u), f(0) = 0, x \in R^n$ and there exists a continuous function $V(x)$, scalars $\varepsilon > 0$, $0 < \kappa < 1$, and $0 < \eta < \infty$ such that*

$$\dot{V}(x) \le -\varepsilon V^{\kappa}(x) + \eta. \tag{14}$$

Then, the trajectory of the nonlinear system is finite-time stable. Therefore, the trajectory of the closed-loop system is bounded in finite time as $\lim_{\theta \longrightarrow \theta_0} x \in (V^{\kappa}(x) \le (\eta/(1-\theta)\varepsilon))$, here $0 < \theta_0 < 1$. And the time to reach such a neighborhood is bounded as

$$T \le \frac{V^{1-\kappa}(x_0)}{\varepsilon^{\theta_0}(1-\kappa)}, \tag{15}$$

where $V(x_0)$ is the initial value of $V(x)$.

Lemma 6 [36]. *For any real number $l_i \in \mathfrak{R}$, $i = 1, \cdots, n$, there exists $0 < p \le 1$ such that*

$$(|l_1| + |l_2| + \cdots + |l_n|)^p \le |l_1|^p + |l_2|^p + \cdots + |l_n|^p. \tag{16}$$

3.2. TSMC-Based Attitude Control System Design. A finite-time attitude control system is designed based on the basic TSMC scheme.

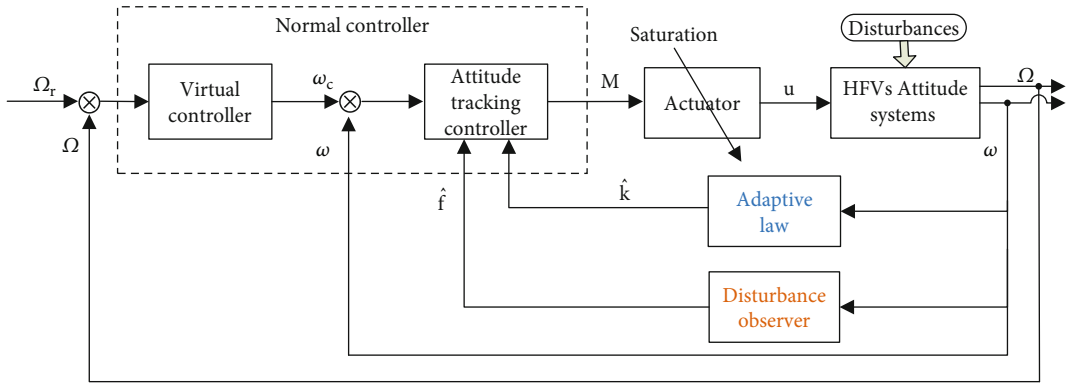

Figure 1: Block diagram of the HFVs attitude control system.

3.2.1. Outer-Loop Controller. A tracking error of outer loop of attitude system is defined as

$$e_1 = \Omega - \Omega_r, \tag{17}$$

where $e_1 \in R^3$ and $\Omega_r \in R^3$ is reference input which can be constant or time-varying. The first fast terminal sliding mode surface is defined as

$$s_1 = \dot{e}_1 + c_1 e_1 + c_2 e_1^{q_1/p_1}, \tag{18}$$

where $s_1 \in R^3$, $c_1 > 1$, c_2 is a positive scalar, and q_1 and p_1 are odd integers satisfying $p_1 > q_1 > 0$. Then, a virtual control law ω_c can be designed as

$$\begin{aligned} \omega_c &= R^{-1}\left(\omega_{eq} + \omega_n\right), \\ \omega_{eq} &= \dot{\Omega}_r - c_1 e_1 - c_2 e_1^{q_1/p_1}, \\ \dot{\omega}_n &= v_1, \\ v_1 &= -k_1 s_1 - \eta_1 \operatorname{sgn}(s_1), \end{aligned} \tag{19}$$

where $\omega_n(0) = 0$; k_1 and η_1 are two positive constants.

3.2.2. Inner-Loop Controller. Similarly, a tracking error of system inner loop is defined as

$$e_2 = \omega - \omega_c, \tag{20}$$

where $e_2 \in R^3$. The second fast terminal sliding mode surface is defined as

$$s_2 = \dot{e}_2 + c_3 e_2 + c_4 e_2^{q_2/p_2}, \tag{21}$$

where $s_2 \in R^3$, $c_3 > 1$, c_4 is a positive scalar, and p_2 and q_2 are odd integers satisfying $p_2 > q_2 > 0$. Then, the TSMC-based attitude control law is designed as

$$\begin{aligned} u &= \left(I^{-1}D\right)^{\dagger}\left(u_{eq} + u_n\right) \\ u_{eq} &= I^{-1}\omega^{\times} I\omega - c_3 e_2 - c_4 e_2^{q_2/p_2} + \dot{\omega}_c, \\ \dot{u}_n &+ T u_n = v_2, \\ v_2 &= -k_2 s_2 - \left(k_d + k_T + \eta_2\right) \operatorname{sgn}(s_2), \end{aligned} \tag{22}$$

where $(I^{-1}D)^{\dagger} = (I^{-1}D)^T\left[(I^{-1}D)(I^{-1}D)^T\right]^{-1}$; $u_n(0) = 0$; k_T, k_2, and η_2 are positive constants; k_d is a constant defined in Assumption 3; and $T \geq 0$ and k_T are selected to satisfy $k_T \geq T l_d$.

Theorem 7. *Consider the HFV attitude system (12) with uncertainties, disturbances, and actuator saturations, suppose that three assumptions are satisfied, the TSMC-based attitude controller (22) guarantees that the attitude angle error e_1 and angular velocity error e_2 converge to zeros in the finite time. Furthermore, the convergent time is calculated by*

$$T_{reach} \leq \frac{V^{1/2}(0)}{\eta\sqrt{2}}. \tag{23}$$

Proof. Choose a Lyapunov function candidate for the closed-loop attitude control system as

$$V = \frac{1}{2} s_1^T s_1 + \frac{1}{2} s_2^T s_2. \tag{24}$$

Substituting the virtual control law (19) into the sliding manifold (18) and differentiating s_1, we have

$$\dot{s}_1 = R\dot{e}_2 + \dot{R}e_2 - k_1 s_1 - \eta_1 \operatorname{sgn}(s_1). \tag{25}$$

Considering the system model (12), the sliding mode manifold (21) can be rewritten as

$$s_2 = -I^{-1}\omega^{\times} I\omega + I^{-1}Du + f - \dot{\omega}_c + c_3 e_2 + c_4 e_2^{q_2/p_2}. \tag{26}$$

Substituting the control law (22) into (26) gives

$$s_2 = -I^{-1}\omega^{\times} I\omega + u_{eq} + u_n + f - \dot{\omega}_c + c_3 e_2 + c_4 e_2^{q_2/p_2} = f + u_n. \tag{27}$$

The solution of (22) is given by

$$u_n(t) = \left(u_n(t_0) + \frac{1}{T}(k_d + k_T + \eta_2)\ \mathrm{sgn}\ (s) + k_2 s_2\right) e^{t-t_0} - \frac{1}{T}((k_d + k_T + \eta_2)\ \mathrm{sgn}\ (s_2) + k_2 s_2). \tag{28}$$

Thus, the following relationship under the condition $u_n(0) = 0$ can be obtained.

$$k_T \geq T l_d \geq T|u_n(t)|_{\max} \geq T|u_n(t)|. \tag{29}$$

For the sliding manifold (21), its derivative with respect to t along system (12) can be obtained as

$$\dot{s}_2 = \frac{d}{dt} f + \dot{u}_n + T u_n - T u_n = \frac{d}{dt} f + v_2 - T u_n. \tag{30}$$

Substituting (22) into (30) gives

$$\dot{s}_2 = \frac{d}{dt} f - (k_d + k_T + \eta_2)\ \mathrm{sgn}\ (s_2) - k_2 s_2 - T u_n. \tag{31}$$

Considering (25) and (31), the time derivative of V is given by

$$\begin{aligned} \dot{V} &= s_1^{\mathrm{T}}\left(R\dot{e}_2 + \dot{R}e_2 - \eta_1\ \mathrm{sgn}\ (s_1) - k_1 s_1\right) \\ &\quad + s_2^{\mathrm{T}}\left(\frac{d}{dt} f - (k_d + k_T + \eta_2)\ \mathrm{sgn}\ (s_2) - k_2 s_2 - T u_n\right) \\ &\leq -\eta_1\|s_1\| - k_1 s_1^{\mathrm{T}} s_1 + \left(s_2^{\mathrm{T}}\frac{d}{dt} f - k_d\|s_2\|\right) \\ &\quad - (T u_n s_2 + k_T\|s_2\|) - \eta_2\|s_2\| - k_2 s_2^{\mathrm{T}} s_2 + s_1^{\mathrm{T}}\left(\dot{R}e_2 + R\dot{e}_2\right) \\ &\leq -\eta_1\|s_1\| - \eta_2\|s_2\| - k_1 s_1^{\mathrm{T}} s_1 - k_2 s_2^{\mathrm{T}} s_2 + s_1^{\mathrm{T}}\left(\dot{R}e_2 + R\dot{e}_2\right). \end{aligned} \tag{32}$$

According to the Young inequality [37], the following inequality can be obtained:

$$s_1^{\mathrm{T}}\dot{R}e_2 \leq \frac{1}{2} s_1^{\mathrm{T}}\dot{R}\dot{R}^{\mathrm{T}} s_1 + \frac{1}{2} e_2^T e_2 \leq \frac{1}{2} s_1^{\mathrm{T}}\dot{R}\dot{R}^{\mathrm{T}} s_1 + \frac{1}{2} s_2^{\mathrm{T}} s_2. \tag{33}$$

Substituting (33) into (32) and assuming the term $R\dot{e}_2$ is bounded satisfying $\|R\dot{e}_2\| \leq \rho$, where ρ is a positive constant, then

$$\dot{V} \leq -(\eta_1 - \rho)\|s_1\| - \eta_2\|s_2\| - s_1^{\mathrm{T}}\left(k_1 I - \frac{1}{2}\dot{R}\dot{R}^{\mathrm{T}}\right) s_1 - \left(k_2 - \frac{1}{2}\right) s_2^{\mathrm{T}} s_2. \tag{34}$$

Let $\eta = \min\{\eta_1 - \rho, \eta_2\}$. By selecting the appropriate k_1, k_2, η_1, and η_2, such that $k_2 > 1/2$, $\eta_1 - \rho > 0$, and $k_1 I - 1/2\dot{R}\dot{R}^{\mathrm{T}} > 0$. Considering Lemma 6, we have

$$\dot{V} \leq -(\eta_1 - \rho)\|s_1\| - \eta_2\|s_2\| \leq -\eta\sqrt{2} V^{1/2} < 0. \tag{35}$$

According to Lemma 4, it is not difficult to find that the sliding manifold s_1 and sliding manifold s_2 converge to zeros in the finite time. Meanwhile, the convergent time is calculated by

$$T_{\mathrm{reach}} \leq \frac{2V^{1/2}(0)}{\eta\sqrt{2}}. \tag{36}$$

This completes the proof of Theorem 7. □

3.3. ATSMC-Based Attitude Control System Design. The TSMC-based attitude controller (22) is designed based on the assumption that the bounds of the uncertainties and their derivatives are known in advance. However, it is difficult to obtain the bound values in advance in some situations, and the switching gain needs to be chosen as a large value to compensate the impact of uncertainties. Unfortunately, the large switching gain may cause large chattering on the sliding surface. To enhance the performance of the HFV attitude control system, an adaptive strategy is employed into the TSMC scheme.

3.3.1. ATSMC-Based Attitude Controller. The ATSMC-based attitude controller is designed as

$$\begin{aligned} u &= \left(I^{-1}D\right)^{\dagger}\left(u_{eq} + u_n\right), \\ u_{eq} &= I^{-1}\omega^{\times} I\omega - c_3 e_2 - c_4 e_2^{q_2/p_2} + \dot{\omega}_c, \\ \dot{u}_n + T u_n &= v_a, \\ v_a &= -k_2 s_2 - \left(\widehat{k} + \eta_2\right)\ \mathrm{sgn}\ (s_2), \end{aligned} \tag{37}$$

where the gain $\widehat{k}$ is the predicted value of the gain $(k_d + k_T)$.

3.3.2. Adaptive Law of the Gain. The gain $\widehat{k}$ is online regulated by an adaptive law:

$$\dot{\widehat{k}} = \frac{1}{\varepsilon}\|s_2\|, \tag{38}$$

where $\varepsilon > 0$ is the adaptation coefficient. The smaller ε will provide a faster convergence but may generate a bigger value than the desired one.

Theorem 8. *Considering the HFV attitude control system (12) with uncertainties, external disturbances, and input saturations, suppose the assumptions are satisfied, the ATSMC-based attitude controller (37) with adaptive law (38) guarantees the system trajectory to reach the sliding surface and remain on it in the finite time, which means that the control system is finite-time stable.*

Proof. Define a Lyapunov function candidate as

$$V = \frac{1}{2}s_1^{\mathrm{T}}s_1 + \frac{1}{2}s_2^{\mathrm{T}}s_2 + \frac{1}{2}\varepsilon\tilde{k}^{\mathrm{T}}\tilde{k}, \tag{39}$$

where the adaptation error $\tilde{k} = \hat{k} - (k_d + k_T)$. Differentiating (39), we have

$$\begin{aligned}\dot{V} = {} & s_1^{\mathrm{T}}\dot{s}_1 + s_2^{\mathrm{T}}\dot{s}_2 + \varepsilon\tilde{k}^{\mathrm{T}}\dot{\tilde{k}} \le -(\eta_1 - \rho)\|s_1\| - k_1 s_1^{\mathrm{T}}s_1 \\ & + s_1^{\mathrm{T}}\dot{R}e_2 - \left(\hat{k} + \eta_2\right)\|s_2\| + s_2^{\mathrm{T}}\frac{d}{dt}(f) - s_2^{\mathrm{T}}Tu_n \\ & - k_2 s_2^{\mathrm{T}}s_2 + \varepsilon\left(\hat{k} - (k_d + k_T)\right)\dot{\hat{k}}.\end{aligned} \tag{40}$$

Substituting the adaptive law (38) into (40) yields

$$\begin{aligned}\dot{V} = {} & -(\eta_1 - \rho)\|s_1\| + s_2^{\mathrm{T}}\frac{d}{dt}(f) - (k_d + k_T + \eta_2)\|s_2\| - s_2^{\mathrm{T}}Tu_n \\ & - k_1 s_1^{\mathrm{T}}s_1 + s_1^{\mathrm{T}}\dot{R}e_2 - k_2 s_2^{T}s_2 \le -(\eta_1 - \rho)\|s_1\| \\ & + \left(s_2^{\mathrm{T}}\frac{d}{dt}(f) - k_d\|s_2\|\right) + \left(-s_2^{\mathrm{T}}Tu_n - k_T\|s_2\|\right) \\ & - \eta_2\|s_2\| \le -(\eta_1 - \rho)\|s_1\| - \eta_2\|s_2\|.\end{aligned} \tag{41}$$

By selecting the appropriate positive constants η_1 and η_2, it is found that $\dot{V} < 0$. Therefore, the attitude conntrol system is asymptotically stable. This implies that the trajectory reaches the sliding surface and remains on it in the finite time. This completes the proof. □

3.4. DO-TSMC-Based Attitude Control System Design. A nonlinear disturbance observer is designed to enhance the disturbance attenuation ability and robustness performance against the uncertainties of the inertia parameters and disturbances. It estimates and compensates for the uncertainties through feedforward, which is no need for prior information of uncertainties.

A new state $\omega_a(t) \in R^3$ is preliminarily introduced with its dynamic satisfying

$$\dot{\omega}_a = -I^{-1}\omega^{\times}I\omega + I^{-1}Du + F\omega_e, \tag{42}$$

where $\omega_e = \omega - \omega_a$ and $F \in R^{3\times3}$ is a constant matrix determined by the design.

3.4.1. Nonlinear Disturbance Observer. A nonlinear disturbance observer is given by

$$\begin{aligned}\dot{\hat{x}} &= -L\hat{x} + L(F\omega_e - P(\omega_e)), \\ \hat{f} &= \hat{x} + P(\omega_e),\end{aligned} \tag{43}$$

where $\hat{f}$ is the estimation of the compound disturbance, $\hat{x}$ is the internal state of the nonlinear observer, $P(\omega_e)$ is a vector-valued function designed as $P(\omega_e) = L\omega_e$, and L is the positive observer gain matrix defined by $L = L^T \in R^{3\times3}$.

Theorem 9. *Considering the HFV attitude dynamics (12) and the nonlinear disturbance observer (43), by selecting a sufficiently large matrix L, the following results can be achieved for all $\tilde{f}(0)$.*

Result 1: the disturbance estimation error $\tilde{f} = f - \hat{f}$ is globally exponentially stable if $\dot{f} = 0$

Result 2: if $\dot{f} \neq 0$ and the rate of change of f is bounded, i.e., there exists a positive scalar $k_d \in R$ such that $\|\dot{f}(t)\| \le k_d$ for all $t \ge 0$, then the disturbance estimation error $\tilde{f}$ converges with an exponential rate, equal to $(1 - \varsigma)(l_{\min} - 1/4)$, where $0 < \varsigma < 1$

Proof. From (12) to (42), it can be obtained that the dynamics of ω_e is such that

$$\dot{\omega}_e = \dot{\omega} - \dot{\omega}_a = f - F\omega_e. \tag{44}$$

In accordance, it follows from (44) that the estimation error $\tilde{f}$ is such that

$$\dot{\tilde{f}} = \dot{f} + L\dot{\hat{x}} - LF\omega_e + LP(\omega_e) - L(f - F\omega_e) = \dot{f} - L\tilde{f}. \tag{45}$$

Considering the following candidate Lyapunov function as $V_1 = 1/2\tilde{f}^{\mathrm{T}}\tilde{f}$, one has

$$\dot{V}_1 = \tilde{f}^{\mathrm{T}}\dot{\tilde{f}} = -\tilde{f}^{\mathrm{T}}L\tilde{f} + \tilde{f}^{\mathrm{T}}\dot{f}. \tag{46}$$

Then, the following two cases are discussed to analyze the stability of $\tilde{f}$.

Case 1: if $\dot{f} = 0$, then (46) can be further simplified as

$$\dot{V}_1 = -\tilde{f}^{T}L\tilde{f} \le -2l_{\min}V_1, \tag{47}$$

where $l_{\min} > 0$ is the minimum eigenvalue of L

Solving (47) yields $V_1(t) \le V_1(0)e^{-2l_{\min}t}$ or

$$\left\|\tilde{f}(t)\right\| \le \sqrt{2V_1(0)}e^{-l_{\min}t}, \tag{48}$$

which implies that the estimation error $\tilde{f}(t)$ will be globally exponential stabilized for any initial observer state, i.e., li $\mathrm{m}_{t\longrightarrow\infty}\|\tilde{f}(t)\| = 0$.

Case 2: if $\dot{f}(t) \neq 0$ and $\|\dot{f}(t)\| \le k_d$, one can get from (46) that

$$\dot{V}_1 \le -l_{\min}\left\|\tilde{f}(t)\right\|^2 + \left\|\tilde{f}(t)\right\|k_d \tag{49}$$

At this stage, by applying the following well-known Young inequality $2a^Tb \le a^Ta + b^Tb, \forall a, b \in R^n$, it can be formulated that

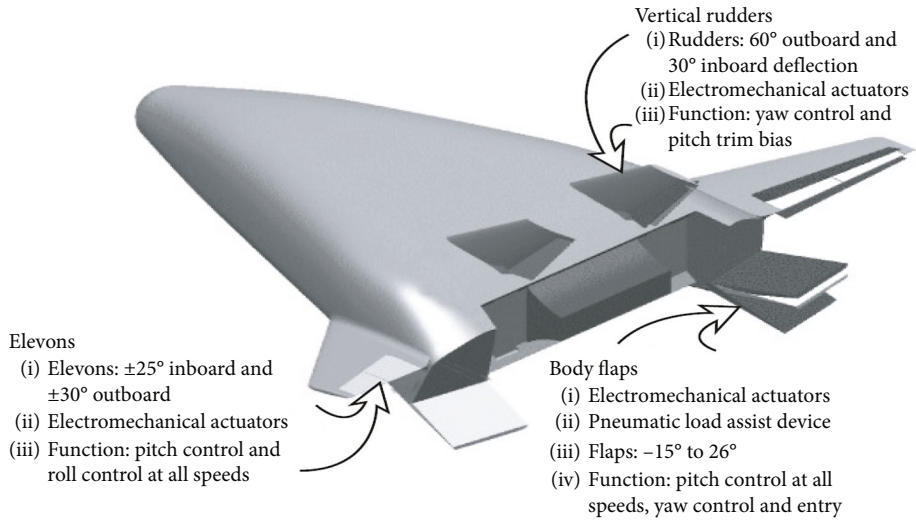

Figure 2: The configuration of the X-33 HFV.

$$\dot{V}_1 \le -\left(l_{\min} - \frac{1}{4}\right)\left\|\tilde{f}(t)\right\|^2 + k_d^2 = -(1-\varsigma)\left(l_{\min} - \frac{1}{4}\right)\left\|\tilde{f}(t)\right\|^2 - \varsigma\left(l_{\min} - \frac{1}{4}\right)\left\|\tilde{f}(t)\right\|^2 + k_d^2, \tag{50}$$

where $0 < \varsigma < 1$ is a positive constant. Therefore,

$$\dot{V}_1 \le -(1-\varsigma)\left(l_{\min} - \frac{1}{4}\right)\left\|\tilde{f}(t)\right\|^2, \forall \|f(t)\| \ge \frac{2k_d}{\sqrt{\varsigma(4l_{\min}-1)}}. \tag{51}$$

To this end, it can be concluded from (51) and the uniform ultimate boundedness theorem that the estimation error $\tilde{f}(t)$ is globally, uniformly, and ultimately bounded.

Moreover, solving the inequality (51), one has

$$V_1(t) \le V_1(0)e^{-2(1-\varsigma)(l_{\min}-1/4)t}, \forall \|f(t)\| \ge \frac{2k_d}{\sqrt{\varsigma(4l_{\min}-1)}}, \tag{52}$$

$$\left\|\tilde{f}(t)\right\| \le \sqrt{2V_1(0)}e^{-(1-\varsigma)(l_{\min}-1/4)t}, \forall \|f(t)\| \ge \frac{2k_d}{\sqrt{\varsigma(4l_{\min}-1)}}. \tag{53}$$

Hence,

$$\left\|\tilde{f}(t)\right\| \le \sqrt{2V_1(0)}e^{-(1-\varsigma)(l_{\min}-1/4)t} + \frac{2k_d}{\sqrt{\varsigma(4l_{\min}-1)}}, \forall t \ge 0. \tag{54}$$

Then, one can conclude that the estimation error $\tilde{f}(t)$ converges with an exponential rate to the ball with radius $2k_d/\sqrt{\varsigma(4l_{\min}-1)}$ for all $\tilde{f}(0)$. □

Table 1: Position limits on the control surface of X-33.

Actuator	Position limit		
	Minimum	Maximum	Unit
Right inboard elevons	-25	+25	Deg
Left inboard elevons	-25	+25	Deg
Right body flaps	-15	+26	Deg
Left body flaps	-15	+26	Deg
Right rudders	-60	+30	Deg
Left rudders	-30	+60	Deg
Right outboard elevons	-30	+30	Deg
Left outboard elevons	-30	+30	Deg

3.4.2. Composite Control Law. The DO-TSMC-based attitude controller is designed as

$$\begin{aligned} u &= \left(I^{-1}D\right)^{\dagger}\left(u_{eq} - \hat{f} + u_n\right), \\ u_{eq} &= I^{-1}\omega^{\times}I\omega - c_3e_2 - c_4e_2^{q_2/p_2} + \dot{\omega}_c, \\ \dot{u}_n &= \nu_b, \\ \nu_b &= -k_3s_2 - \eta_3\ \mathrm{sgn}\ (s_2), \end{aligned} \tag{55}$$

where $\hat{f}$ is the estimate of f which can be obtained by the observer (43), $u_n(0) = 0$, and η_3 and k_3 are positive constants.

Theorem 10. *Considering the HFV attitude system (12), the DO-TSMC-based attitude controller (55) with the nonlinear disturbance observer (43) and the virtual controller (19) can guarantee that the attitude angle error e_1 and angular velocity error e_2 converge to zeros in the finite time.*

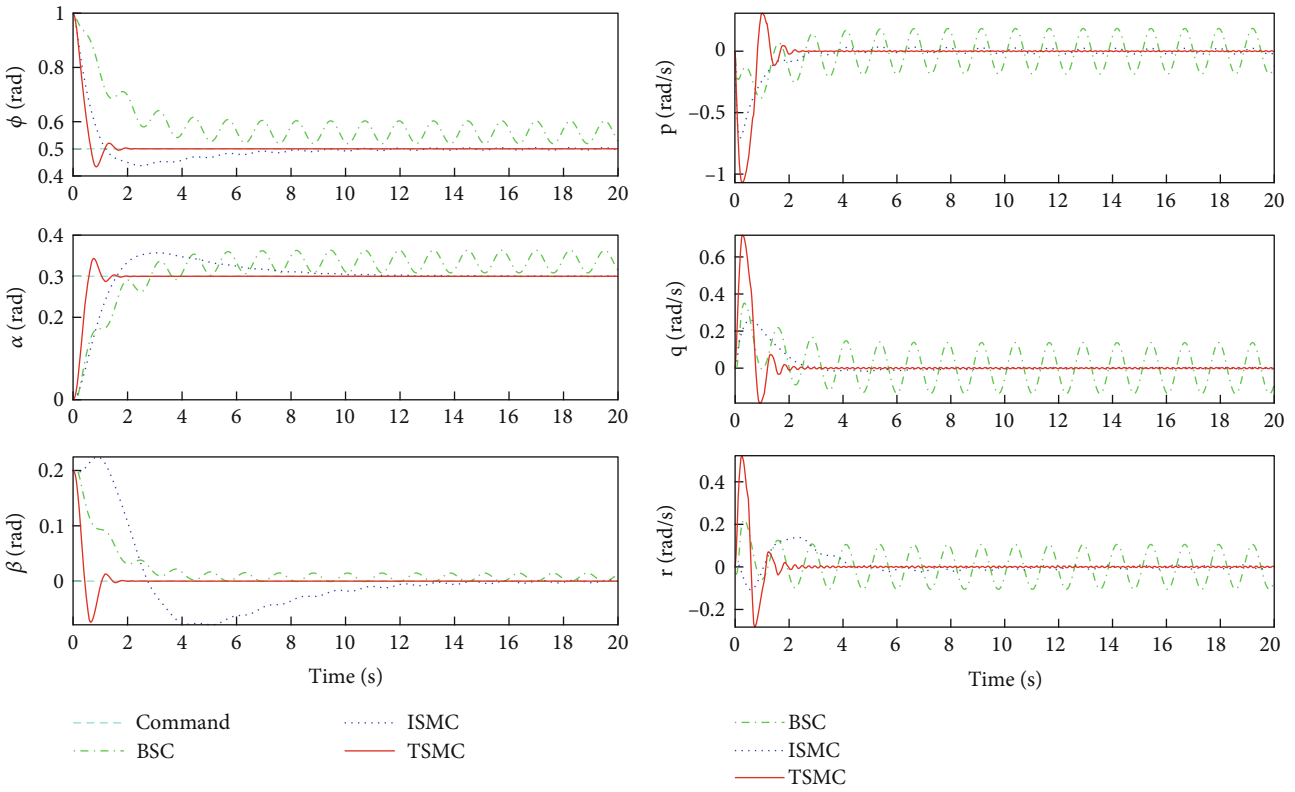

Figure 3: Attitude angle and angular rate responses under different methods.

Proof. Choose the Lyapunov function candidate for the closed-loop attitude control systems as

$$V = \frac{1}{2}s_1^{\mathrm{T}}s_1 + \frac{1}{2}s_2^{\mathrm{T}}s_2. \tag{56}$$

Differentiating (56), substituting (25), (31), and (55), it leads to

$$\dot{V} = s_1^{\mathrm{T}}\left(-\eta_1\ \mathrm{sgn}\ (s_1) - k_1 s_1 + R\dot{e}_2 + \dot{R}e_2\right) + s_2^{\mathrm{T}}\left(\dot{\tilde{f}} - \eta_3\ \mathrm{sgn}\ (s_2) - k_3 s_2\right). \tag{57}$$

According to the Young inequality, the following inequalities can be obtained:

$$s_2^{\mathrm{T}}\dot{\tilde{f}} \le \frac{1}{2}s_2^{\mathrm{T}}s_2 + \frac{1}{2}\dot{\tilde{f}}^{\mathrm{T}}\dot{\tilde{f}} = \frac{1}{2}\left(\|s_2\|^2 + \left\|\dot{\tilde{f}}\right\|^2\right). \tag{58}$$

Substituting (58) and (33) into (57) and selecting the appropriate k_1, k_3, η_1, and η_2, such that $k_3 > 1$, $\eta_1 - \rho > 0$, and $k_1 I - 1/2\dot{R}\dot{R}^{\mathrm{T}} > 0$, it further has

$$\dot{V} \le -(\eta_1 - \rho)\|s_1\| - \eta_3\|s_2\| + \varpi, \tag{59}$$

where $\varpi = 1/2\|\dot{\tilde{f}}\|^2 > 0$. Let $\chi = \min\{\eta_1 - \rho, \eta_3\}$. 6, we have

$$\dot{V} \le -\chi\sqrt{2}V^{1/2} + \varpi. \tag{60}$$

According to Lemma 5, it is not difficult to find that the sliding manifold s_1 and sliding manifold s_2 converge to zero in the finite time. This completes the proof of Theorem 10. □

Remark 11. In terms of singular perturbation theory, the inner-loop sliding mode dynamics in (21) must be much faster than the outer-loop sliding mode dynamics in (18) to preserve sufficient time-scale separation between two loops.

Remark 12. In the HFV attitude control system, since the control system keeps the sideslip angle $\beta = 0°$ during the reentry phase, it is assumed that the singular situation ($\beta = \pm 90°$) will not occur. Moreover, only v_2, v_a, and v_b contain switch terms, while the actual control u does not contain these terms. In the designed controller (22), $\dot{u}_n + Tu_n = v_2$ is equal to a low-pass filter with the bandwidth of T, where v_2 is input signal and u_n is output signal. The Laplace transformation of it is given by $(u_n(s)/v_2(s)) = (1/s + T)$. Although v_2 is chattering because of the switch function, u_n can be smoothed due to the low-pass filter, which can eliminate the impact of chattering on the system. In particular case, $T = 0$, such as the designed controller (55), $\dot{u}_n = v_b$ is same as a pure integrator, which can also soften the sgn (s_2) signal. In addition, the introduction of adaptive mechanism and disturbance observer can make the sign function gain selection very small. Therefore, the proposed control methods are chattering-free.

Remark 13. Most disturbance observers are designed on the assumption that the disturbance value is a constant or a

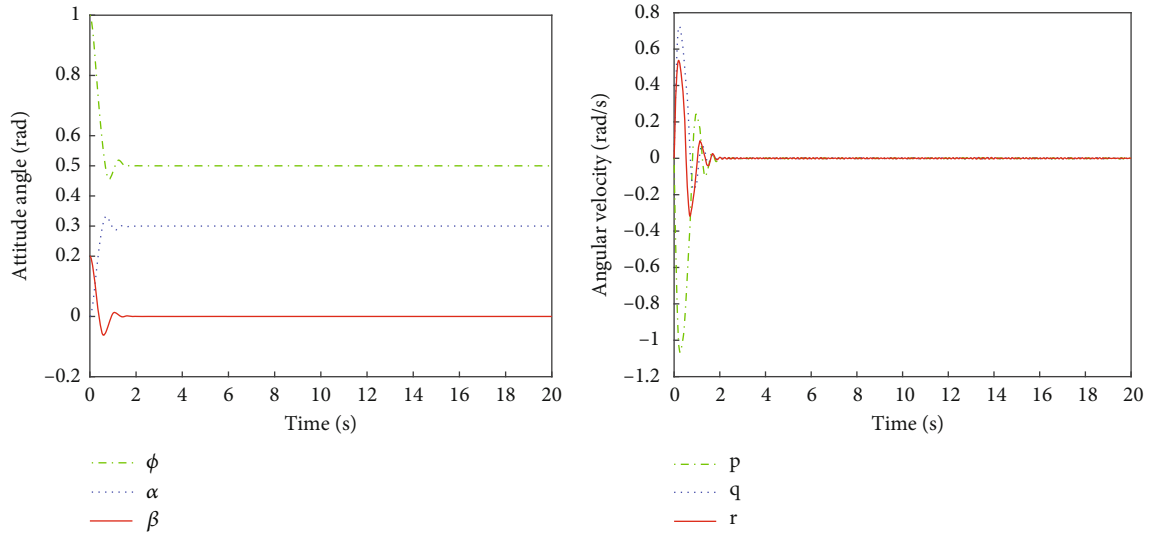

Figure 4: Attitude angle and angular rate responses under ATSMC.

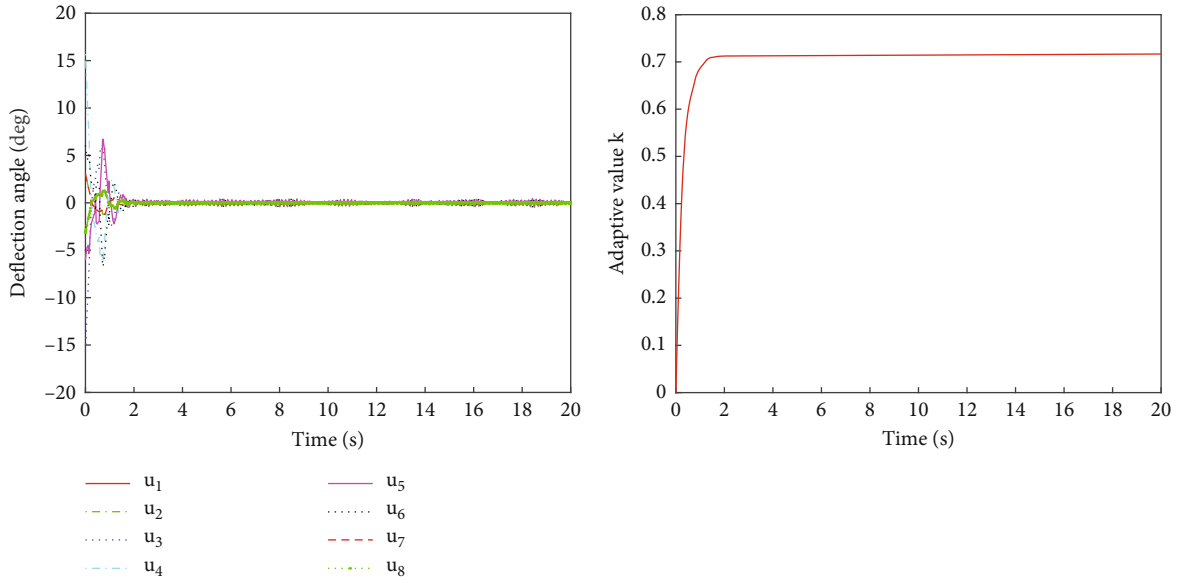

Figure 5: Control surface deflection and adaptive value responses under ATSMC.

slowly varying [34], i.e., $\dot{f} = 0$, $\dot{f} \approx 0$, or $\lim_{t \to \infty} \dot{f} = 0$. The designed nonlinear disturbance observer can release the restrictions on the change speed of the lumped disturbance and prove that the estimation error of the lumped disturbance is exponentially convergent.

4. Simulation Study

In this study, the proposed finite-time attitude tracking control algorithms are applied to a generic nonlinear model of X-33 HFV, and a MATLAB/Simulink-based thorough simulation study is conducted to show some insights in the nonlinear system.

4.1. Parameters of HFV Model and Attitude Control System

4.1.1. HFV Model. In this section, we choose the X-33 HFV as the controlled plant and the parameters of this model refer to reference [34]. Figure 2 shows the configuration of the X-33 HFV [31, 38]. Its weight is 136078 kg, and it is equipped with four sets of control surfaces. Each control surface can be independently actuated with one actuator, i.e., rudders, body flaps, and inboard and outboard elevons, respectively, with left and right sides for each set. The selection of matrix $D \in R^{3\times 8}$ refers to reference [34, 39]. Hence, the control input vector is $u = [u_1, u_2, u_3, u_4, u_5, u_6, u_7, u_8]^T$, where u_1 and u_2 are the right and left inboard elevons, u_3 and u_4 are the right and left body

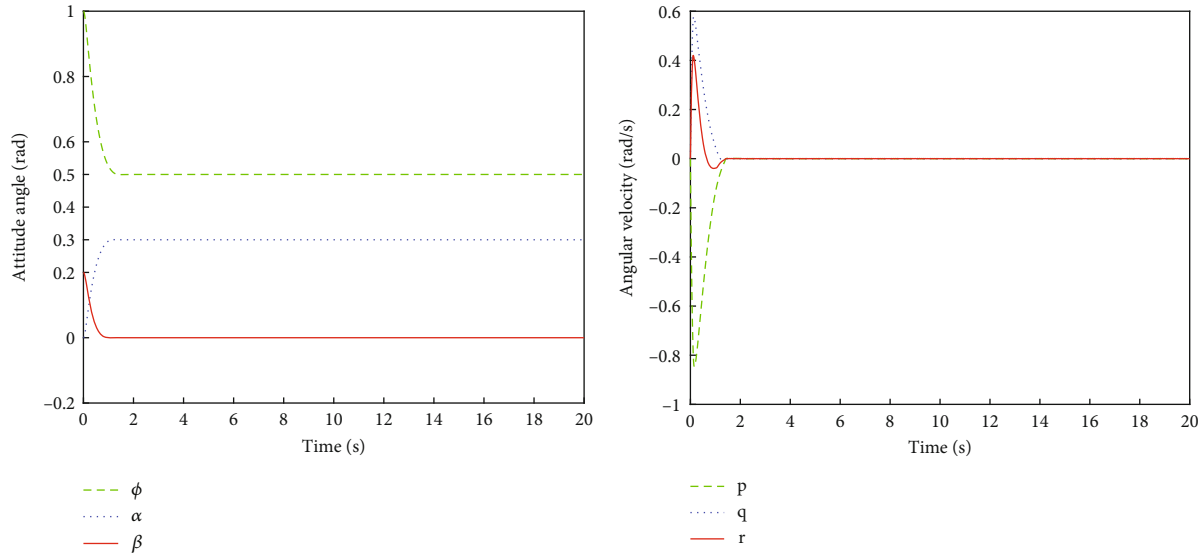

Figure 6: Attitude angle and its angular rate responses under DO-TSMC.

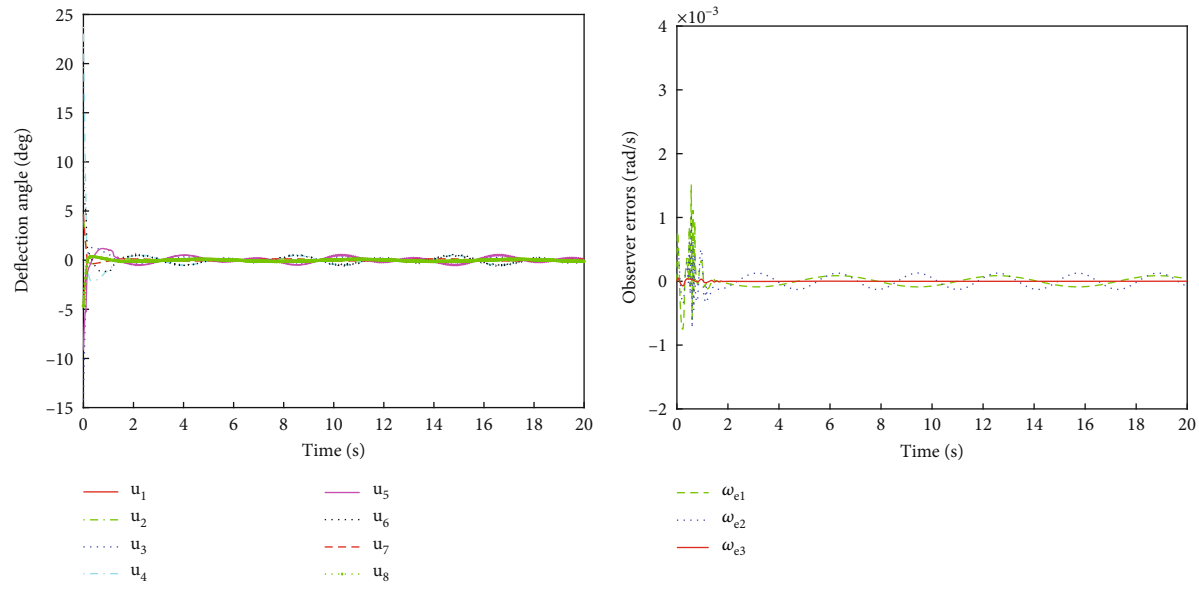

Figure 7: Control surface deflection and observer error responses under DO-TSMC.

flaps, u_5 and u_6 are the right and left rudders, and u_7 and u_8 are the right and left outboard elevons, respectively. The actuator position limits of the X-33 vehicle are listed in Table 1. The moment of inertia tensor and parameter uncertainties are given by

$$I = \begin{pmatrix} 554486 & 0 & -23002 \\ 0 & 1136949 & 0 \\ -23002 & 0 & 1376852 \end{pmatrix},$$
$$\Delta I = \begin{pmatrix} -500 & 0 & 0 \\ 0 & -500 & 0 \\ 0 & 0 & -500 \end{pmatrix}. \quad (61)$$

Furthermore, the external disturbances of the NSV are assumed as

$$d(\mathrm{t}) = \begin{bmatrix} d_1(\mathrm{t}) \\ d_2(\mathrm{t}) \\ d_3(\mathrm{t}) \end{bmatrix} = \begin{bmatrix} 160000(\sin(5\mathrm{t}) + 0.25) \\ 25000(\sin(5\mathrm{t}) + 0.20) \\ 25000(\sin(5\mathrm{t}) + 0.10) \end{bmatrix}. \quad (62)$$

4.1.2. Control Commands and Control Schemes. Assume that the HFV is flying with velocity of 2500 m/s and height of 40000 m. The initial attitude angles are that $\phi = 1$rad, $\alpha = 0$ rad, $\beta = 0.2$rad, and $p = q = r = 0(\mathrm{rad/s})$. The HFV attitude tracking commands are given as $\phi_r = 0.5$rad, $\alpha_r = 0.3$rad, and $\beta_r = 0$rad. The effectiveness of the TSMC scheme is verified by comparing with a backstepping control (BSC) method

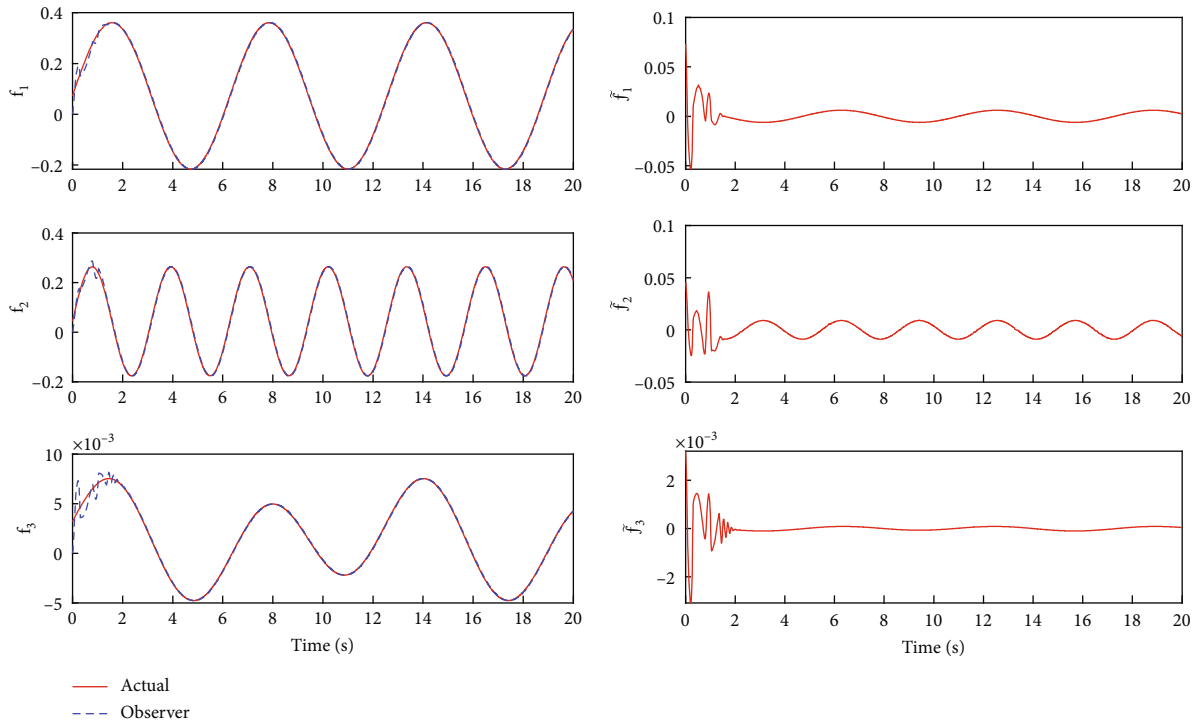

Figure 8: Disturbance estimate and estimation error responses under DO-TSMC.

[30] and an integral sliding mode control (ISMC) method [32]. Furthermore, the effectiveness of the ATSMC and DO-TSMC is also verified. For the BSC, $\Lambda_1 = \text{diag}\{25,25,25\}$ and $\Lambda_2 = \text{diag}\{25,25,25\}$. For the ISMC, $K_1 = \text{diag}\{0.4,0.4,0.4\}$, $K_2 = \text{diag}\{1.88,1.88,1.88\}$, $\rho = \text{diag}\{1,0.15,0.08\}$, and $\widehat{\rho} = \text{diag}\{4.0 \times 10^6, 4.0 \times 10^6, 4.0 \times 10^6\}$. For the TSMC, $p_1 = 3$, $q_1 = 1$, $p_2 = 7$, $q_2 = 5$, $c_1 = 2$, $c_2 = 3$, $c_3 = 7$, $c_4 = 10$, $k_1 = 15$, $k_2 = 10.5$, $\eta_1 = 0.1$, $\eta_2 = 0.4$, $k_d + k_T = 15$, and $T = 0.5$. For the ATSMC, $p_1 = 3$, $q_1 = 1$, $p_2 = 4$, $q_2 = 5$, $c_1 = 2$, $c_2 = 3$, $c_3 = 7$, $c_4 = 10$, $k_1 = 15$, $k_2 = 10.5$, $\eta_1 = 0.1$, $\eta_2 = 0.4$, $T = 0.5$, and $\gamma = 0.4$. For the DO-TSMC, $p_1 = 3$, $q_1 = 1$, $p_2 = 7$, $q_2 = 5$, $c_1 = 2$, $c_2 = 3$, $c_3 = 7$, $c_4 = 10$, $k_1 = 15$, $k_2 = 10.5\eta_1 = 0.1$, $\eta_3 = 0.2$, and $L = \text{diag}\{105,105,105\}$.

4.2. Simulation Results and Discussion. The comparisons on the tracking performance of attitude angle and angular rate as well as actuator inputs using the BSC, ISMC, and TSMC schemes are shown in Figure 3. The responses of the attitude angles and angular velocities by the ATMC method are shown in Figure 4. And Figure 5 shows the control surface deflections and adaptive value responses. Figure 6 shows the tracking responses of the attitude angles and angular rates under DO-TSMC scheme, and Figure 7 gives the control surface deflections and observer estimation error responses. Figure 8 shows the lumped disturbance estimation and estimation error responses under DO-TSMC.

4.2.1. Comparison between the TSMC, BSC, and ISMC Methods. The proposed TSMC method as a finite-time sliding mode control method is compared with the traditional BSC and ISMC methods for the NSV system. Viewing from Figures 3 and 9, the attitude angle outputs cannot satisfactorily track the desired commands with large tracking errors and even cannot be stable by using the BSC method. Although the ISMC can make the system outputs track the desired commands, it needs a longer settling time than the TSMC method. As shown in Figure 9, affected by the disturbance, all control surfaces of the BSC system are in a large range of changes, which will cause a lot of energy loss. Due to the limited output of the actuator, it can be seen from the response of u_3 that the right body flaps have been at the minimum deflection angle (−15 deg) for about 0.2 seconds. After the adjustment of the TSMC controller, the output of the actuator has been in a reasonable small range. As shown in Figure 9, the left body flap u_4 of BSC system is always at the minimum deflection angle (−15 deg) at 0.25-0.4 second, resulting in actuator saturation. In all, the TSMC scheme obviously has the best performance than the BSC scheme and ISMC scheme, for the attitude control problem with model uncertainties, external disturbances, and actuator saturations.

4.2.2. Comparison between the ATMC and TSMC Methods. The ATMC applies an adaptive mechanism to relax the bounded lumped disturbance information of the basic TSMC. Figure 4 shows that the ATMC scheme can stabilize the attitude angles and angular rates in the finite time. For the TSMC, when the system lacks the upper bound information, a larger switching gain will be chosen that may lead to large chattering on the control surface. For the ATMC, the control chattering problem is effectively attenuated due to the adaptive mechanism. As shown in Figure 5, the predicted value of the gain $k_d + k_T$ can converge to the constant 0.7 in a very short time.

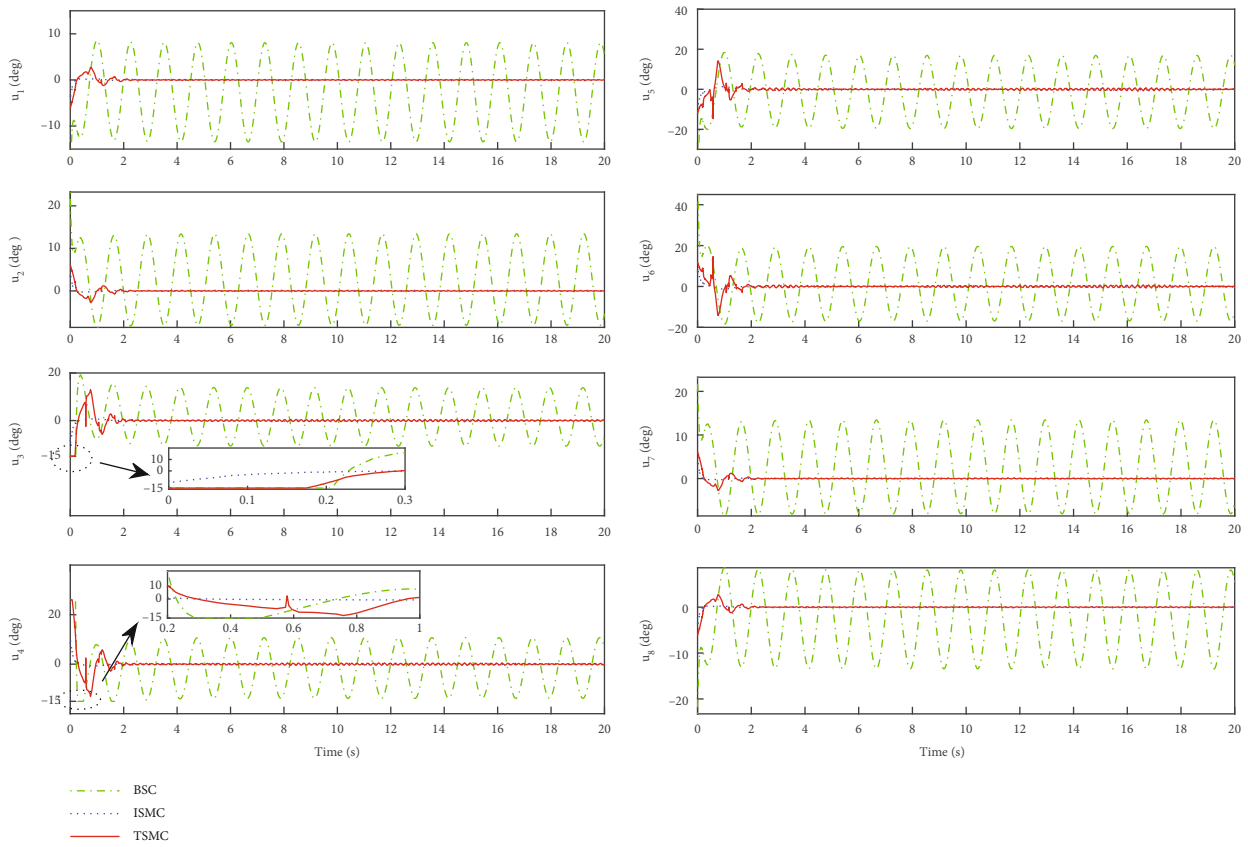

Figure 9: Control surface deflection responses.

Therefore, the ATSMC scheme achieves a good performance even though the system uncertainty bounds are unknown in advance.

4.2.3. Comparison between the DO-TMC and TSMC Methods. The DO-TMC applies a nonlinear disturbance observer to relax the restrictions of lumped disturbance and attenuate chattering phenomenon of the basic TSMC. For the DO-TMC, the HFV attitude system smoothly achieves stabilization with a settling time less than 1.5 s and a high accuracy, as shown in Figure 6. By selecting the appropriate values of the disturbance observer parameters, it can be seen from Figure 7 that the observer error ω_e can converge to a very small interval, i.e., $|\omega_{ei}| \leq 2 \times 10^{-3}$. The estimated information of the observer is transmitted to the controller to adjust the output of the actuator in real time, so that each control surface can deflect in a small range. Figure 8 shows the estimated response curve and estimation error curve under the proposed disturbance observer. Figure 8 exhibits that the proposed observer has good performance on the estimated slow time varying, fast time varying, and periodic disturbance. Above all, the DO-TSMC scheme can significantly achieve a satisfied performance without any prior knowledge of the compound uncertainties of the HFV control system.

5. Conclusion

In this study, three finite-time attitude tracking control schemes (TSMC, ATSMC, and DO-TSMC) have been designed for the attitude control problem of nonlinear HFV with model uncertainties, external disturbances, and actuator saturations. The ATSMC scheme is based on combination of the TSMC and an adaptation law, while the DO-TSMC scheme is based on the combination of the TSMC and a nonlinear disturbance observer. Meanwhile, the stability of the closed-loop attitude system is analyzed using the Lyapunov function theory. The simulation results of a nonlinear X-33 HFV model show that the TSMC scheme has a better performance than the traditional BSC and ISMC schemes, the ATSMC scheme achieves a satisfied performance in case of unknown bounds of the compound uncertainties, and the DO-TSMC scheme improves the robustness and disturbance rejection performance of the attitude control system.

This work considers the uncertainties, disturbances, and actuator saturations of the HFV system, which will contribute to the practical applications and better control performance. However, the actuator faults such as stuck or loss of effectiveness are not considered, which will be one of the subjects for future research.

Data Availability

All simulation data in this study are included within the article.

Conflicts of Interest

The authors declare that they have no conflicts of interest.

Acknowledgments

This work is supported in part by the Postgraduate Research & Practice Innovation Program of Jiangsu Province (No. KYCX18_0299). The authors also gratefully acknowledge the financial support from the program of China Scholarship Council (No. 201806830102).

References

[1] S. Liang, B. Xu, and J. Ren, "Kalman-filter-based robust control for hypersonic flight vehicle with measurement noises," *Aerospace Science and Technology*, vol. 112, article 106566, 2021.

[2] Z. Guo, J. Guo, J. Zhou, and J. Chang, "Robust tracking for hypersonic reentry vehicles via disturbance estimation-triggered control," *IEEE Transactions on Aerospace and Electronic Systems*, vol. 56, no. 2, pp. 1279–1289, 2020.

[3] Y. Li, S. Liang, B. Xu, and M. Hou, "Predefined-time asymptotic tracking control for hypersonic flight vehicles with input quantization and faults," *IEEE Transactions on Aerospace and Electronic Systems*, vol. 57, no. 5, pp. 2826–2837, 2021.

[4] Z. Dong, Y. Li, M. Lv, and R. Zuo, "Adaptive accurate tracking control of HFVs in the presence of dead-zone and hysteresis input nonlinearities," *Chinese Journal of Aeronautics*, vol. 34, no. 5, pp. 642–651, 2021.

[5] X. Shao, Y. Shi, W. Zhang, and J. Zhao, "Prescribed fast tracking control for flexible air-breathing hypersonic vehicles: an event-triggered case," *Chinese Journal of Aeronautics*, vol. 34, no. 11, pp. 200–215, 2021.

[6] X. Bu and Q. Qi, "Fuzzy optimal tracking control of hypersonic flight vehicles via single-network adaptive critic design," *IEEE Transactions on Fuzzy Systems*, vol. 30, no. 1, pp. 270–278, 2022.

[7] L. Dou, M. Du, Q. Mao, and Q. Zong, "Finite-time nonsingular terminal sliding mode control-based fuzzy smooth-switching coordinate strategy for AHV-VGI," *Aerospace Science and Technology*, vol. 106, article 106080, 2020.

[8] X. Liang, Q. Wang, C. Hu, and C. Dong, "Fixed-time observer based fault tolerant attitude control for reusable launch vehicle with actuator faults," *Aerospace Science and Technology*, vol. 107, article 106314, 2020.

[9] S. Liu, Y. Sang, and J. F. Whidborne, "Adaptive sliding-mode-backstepping trajectory tracking control of underactuated airships," *Aerospace Science and Technology*, vol. 97, article 105610, 2020.

[10] T. Han, Q. Hu, H. S. Shin, A. Tsourdos, and M. Xin, "Incremental twisting fault tolerant control for hypersonic vehicles with partial model knowledge," *IEEE Transactions on Industrial Informatics*, vol. 18, no. 2, pp. 1050–1060, 2022.

[11] K. Chen, S. Zhu, C. Wei, T. Xu, and X. Zhang, "Output constrained adaptive neural control for generic hypersonic vehicles suffering from non-affine aerodynamic characteristics and stochastic disturbances," *Aerospace Science and Technology*, vol. 111, article 106469, 2021.

[12] Z. Guo, Q. Ma, J. Guo, B. Zhao, and J. Zhou, "Performance-involved coupling effect-triggered scheme for robust attitude control of HRV," *IEEE/ASME Transactions on Mechatronics*, vol. 25, no. 3, pp. 1288–1298, 2020.

[13] Y. Gao, J. Liu, Z. Wang, and L. Wu, "Interval type-2 FNN-based quantized tracking control for hypersonic flight vehicles with prescribed performance," *IEEE Transactions on Systems, Man, and Cybernetics: Systems*, vol. 51, no. 3, pp. 1981–1993, 2021.

[14] J. Zhang, J. D. Biggs, D. Ye, and Z. Sun, "Finite-time attitude set-point tracking for thrust-vectoring spacecraft rendezvous," *Aerospace Science and Technology*, vol. 96, article 105588, 2020.

[15] Y. Lu, "Disturbance observer-based backstepping control for hypersonic flight vehicles without use of measured flight path angle," *Chinese Journal of Aeronautics*, vol. 34, no. 2, pp. 396–406, 2021.

[16] Y. Li, M. Hou, S. Liang, and G. Jiao, "Predefined-time adaptive fault-tolerant control of hypersonic flight vehicles without overparameterization," *Aerospace Science and Technology*, vol. 104, article 105987, 2020.

[17] J. Sun, J. Yi, Z. Pu, and Z. Liu, "Adaptive fuzzy nonsmooth backstepping output-feedback control for hypersonic vehicles with finite-time convergence," *IEEE Transactions on Fuzzy Systems*, vol. 28, no. 10, pp. 2320–2334, 2020.

[18] Y. Shou, B. Xu, X. Liang, and D. Yang, "Aerodynamic/reaction-jet compound control of hypersonic reentry vehicle using sliding mode control and neural learning," *Aerospace Science and Technology*, vol. 111, article 106564, 2021.

[19] X. Yu, P. Li, and Y. Zhang, "Fixed-time actuator fault accommodation applied to hypersonic gliding vehicles," *IEEE Transactions on Automation Science and Engineering*, vol. 18, no. 3, pp. 1429–1440, 2021.

[20] Y. Zhang, Y. Shou, P. Zhang, and W. Han, "Sliding mode based fault-tolerant control of hypersonic reentry vehicle using composite learning," *Neurocomputing*, vol. 484, pp. 142–148, 2022.

[21] F. Wang, Y. Li, C. Zhou, Q. Zong, and C. Hua, "Composite practically fixed time controller design for a hypersonic vehicle with multisource uncertainty and actuator fault," *IEEE Transactions on Aerospace and Electronic Systems*, vol. 57, no. 6, pp. 4375–4389, 2021.

[22] J. Sun, J. Yi, Z. Pu, and X. Tan, "Fixed-time sliding mode disturbance observer-based nonsmooth backstepping control for hypersonic vehicles," *IEEE Transactions on Systems, Man, and Cybernetics: Systems*, vol. 50, no. 11, pp. 4377–4386, 2020.

[23] J. Sun, Z. Pu, J. Yi, and Z. Liu, "Fixed-time control with uncertainty and measurement noise suppression for hypersonic vehicles via augmented sliding mode observers," *IEEE Transactions on Industrial Informatics*, vol. 16, no. 2, pp. 1192–1203, 2020.

[24] T. Cao, H. Gong, P. Cheng, and Y. Xue, "A novel learning observer-based fault-tolerant attitude control for rigid spacecraft," *Aerospace Science and Technology*, vol. 128, article 107751, 2022.

[25] Y. Lu, Z. Jia, X. Liu, and K. Lu, "Output feedback fault-tolerant control for hypersonic flight vehicles with non-affine actuator faults," *Acta Astronautica*, vol. 193, pp. 324–337, 2022.

[26] V. Tharanidharan, R. Sakthivel, Y. Ma, L. Susana Ramya, and S. Marshal Anthoni, "Finite-time decentralized non-fragile dissipative control for large-scale systems against actuator saturation," *ISA Transactions*, vol. 91, pp. 90–98, 2019.

[27] M. Chen, Q. Wu, C. Jiang, and B. Jiang, "Guaranteed transient performance based control with input saturation for near space vehicles," *SCIENCE CHINA Information Sciences*, vol. 57, no. 5, pp. 1–12, 2014.

[28] J. Sun, S. Xu, S. Song, and X. Dong, "Finite-time tracking control of hypersonic vehicle with input saturation," *Aerospace Science and Technology*, vol. 71, pp. 272–284, 2017.

[29] Y. Ding, X. Yue, C. Liu, H. Dai, and G. Chen, "Finite-time controller design with adaptive fixed-time anti-saturation compensator for hypersonic vehicle," *ISA Transactions*, vol. 122, pp. 96–113, 2022.

[30] Q. Hu and Y. Meng, "Adaptive backstepping control for air-breathing hypersonic vehicle with actuator dynamics," *Aerospace Science and Technology*, vol. 67, pp. 412–421, 2017.

[31] Z. Gao, B. Jiang, and P. Shi, "Active fault tolerant control design for reusable launch vehicle using adaptive sliding mode technique," *Journal of the Franklin Institute*, vol. 349, no. 4, pp. 1543–1560, 2012.

[32] Y. Shtessel, C. Hall, and M. Jackson, "Reusable launch vehicle control in multiple-time-scale sliding modes," *Journal of Guidance Control Dynamics (Pembroke, Ont.)*, vol. 23, no. 6, pp. 1013–1020, 2000.

[33] J. Song, Y. Niu, and Y. Zou, "Finite-time sliding mode control synthesis under explicit output constraint," *Automatica*, vol. 65, pp. 111–114, 2016.

[34] D. Xu, B. Jiang, and P. Shi, "Robust NSV fault-tolerant control system design against actuator faults and control surface damage under actuator dynamics," *IEEE Transactions on Industrial Electronics*, vol. 62, no. 9, pp. 5919–5928, 2015.

[35] Q. Shen, D. Wang, S. Zhu, and K. Poh, "Finite-time fault-tolerant attitude stabilization for spacecraft with actuator saturation," *IEEE Transactions on Aerospace and Electronic Systems*, vol. 51, no. 3, pp. 2390–2405, 2015.

[36] J. Zhang, Q. Hu, and D. Wang, "Bounded finite-time attitude tracking control for rigid spacecraft via output feedback," *Aerospace Science and Technology*, vol. 64, pp. 75–84, 2017.

[37] K. Sun, S. Sui, and S. Tong, "Optimal adaptive fuzzy FTC design for strict-feedback nonlinear uncertain systems with actuator faults," *Fuzzy Sets and Systems*, vol. 316, pp. 20–34, 2017.

[38] S. Patrick, I. Michael, and O. Michael, "Faut-tolerant optimal trajectory generation for renusable launch vehicles," *Journal of Guidance Control Dynamics (Pembroke, Ont.)*, vol. 30, no. 6, pp. 1794–1802, 2007.

[39] B. Hollis, R. Nowak, R. Thompson et al., "X-33 aerodynamic and aeroheating computations for wind tunnel and flight conditions," in *24th Atmospheric Flight Mechanics Conference*, Portland,OR,U.S.A, 1999.